Supplement of

Combined assimilation of NOAA surface and MIPAS satellite observations to constrain the global budget of carbonyl sulfide

Jin Ma[1], Linda M. J. Kooijmans[2], Norbert Glatthor[3], Stephen A. Montzka[4], Marc von Hobe[5], Thomas Röckmann[1], and Maarten C. Krol[1,2]

[1]Institute for Marine and Atmospheric Research, Utrecht University, Utrecht, The Netherlands
[2]Meteorology and Air Quality, Wageningen University & Research, Wageningen, The Netherlands
[3]Institute of Meteorology and Climate Research, Karlsruhe Institute of Technology, Karlsruhe, Germany
[4]National Oceanic and Atmospheric Administration (NOAA), Boulder, CO, USA
[5]Forschungszentrum Jülich GmbH, Germany

Correspondence: Jin Ma (j.ma@uu.nl)

The supplement material contains additional figures, which are referred to in the main text with a capital S.

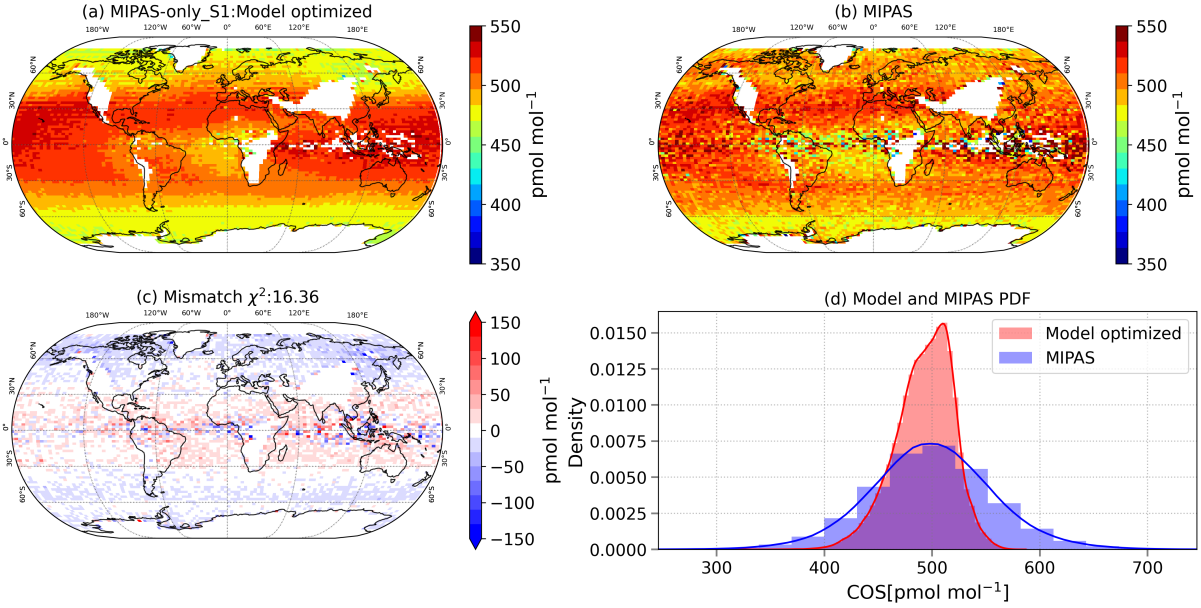

Figure S1. Comparison of inversion MIPAS_only_S1 with MIPAS data: (a) modelled COS; (b) MIPAS data (level 8); (c) mismatch (a) minus (b). The χ^2 value, without accounting error inflation, is given in the header (d) probability density function of modelled and MIPAS mixing ratios.

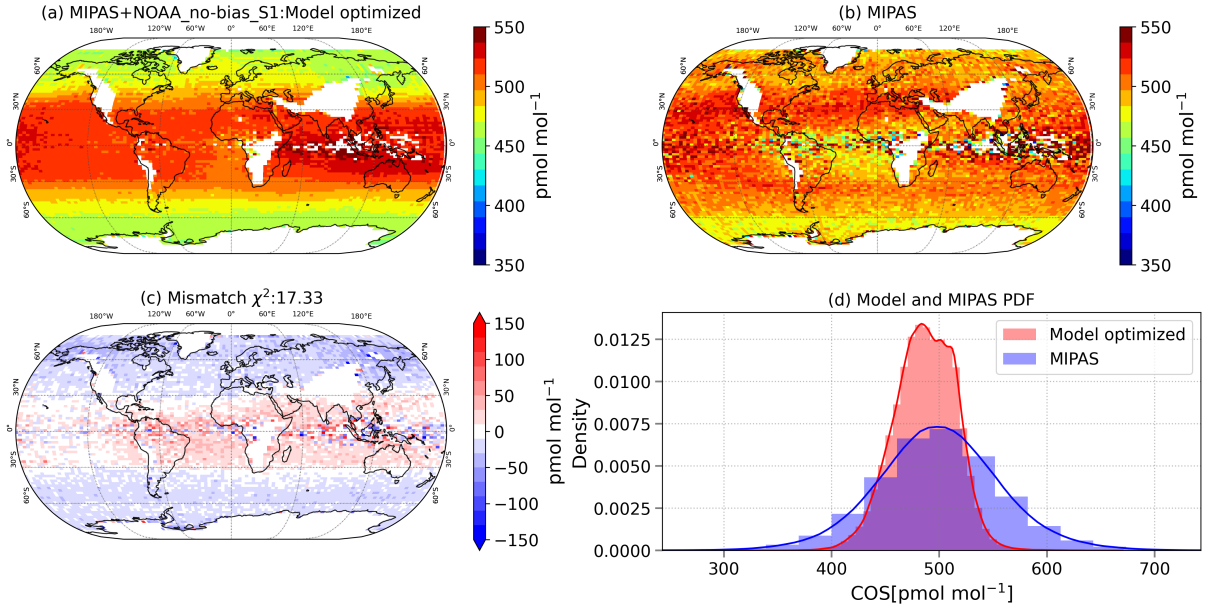

Figure S2. Comparison of inversion MIPAS+NOAA_no-bias_S1 with MIPAS data: (a) modelled COS; (b) MIPAS data (level 8); (c) mismatch (a) minus (b). The χ^2 value, without accounting for error inflation, is given in the header (d) probability density function of modelled and MIPAS mixing ratios.

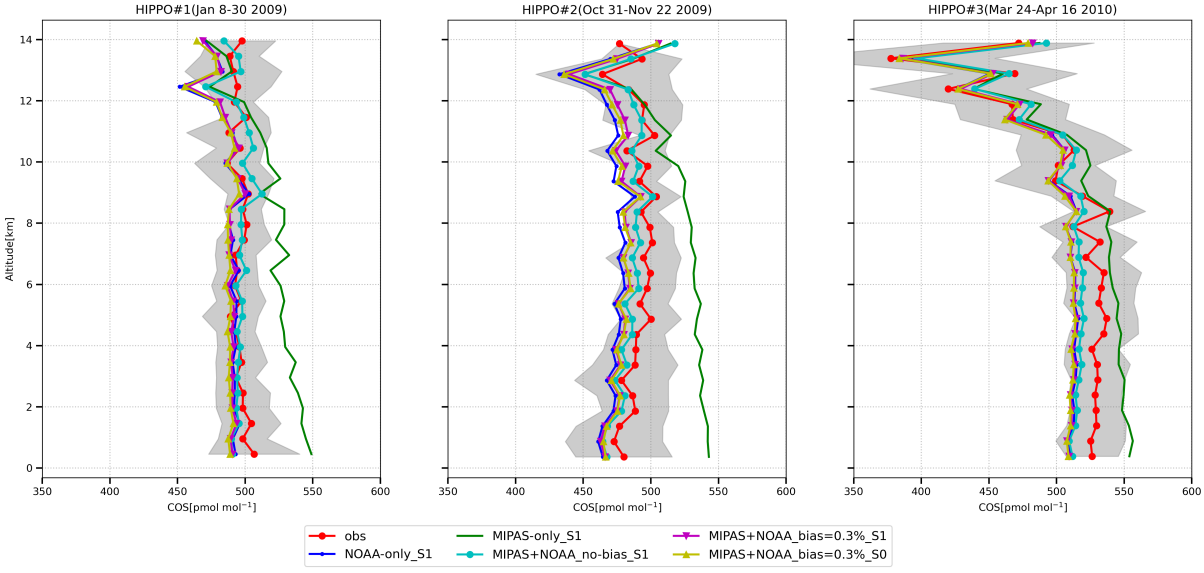

Figure S3. Vertical profiles of HIPPO observations and inversions. The profiles were averaged each 500 m vertically. HIPPO campaigns 1–3 are shown. The gray shading is the standard deviation of the observations that are shown in red.

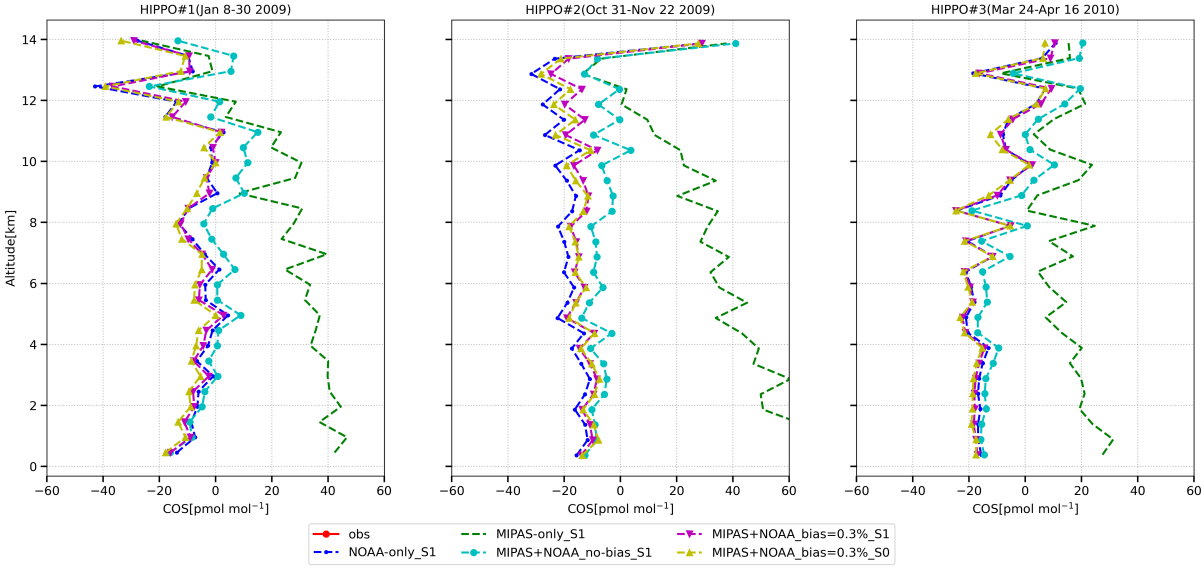

Figure S4. Differences between vertical profiles of HIPPO observations and inversions. The profiles were averaged each 500 m vertically. HIPPO campaigns 1–3 are shown.

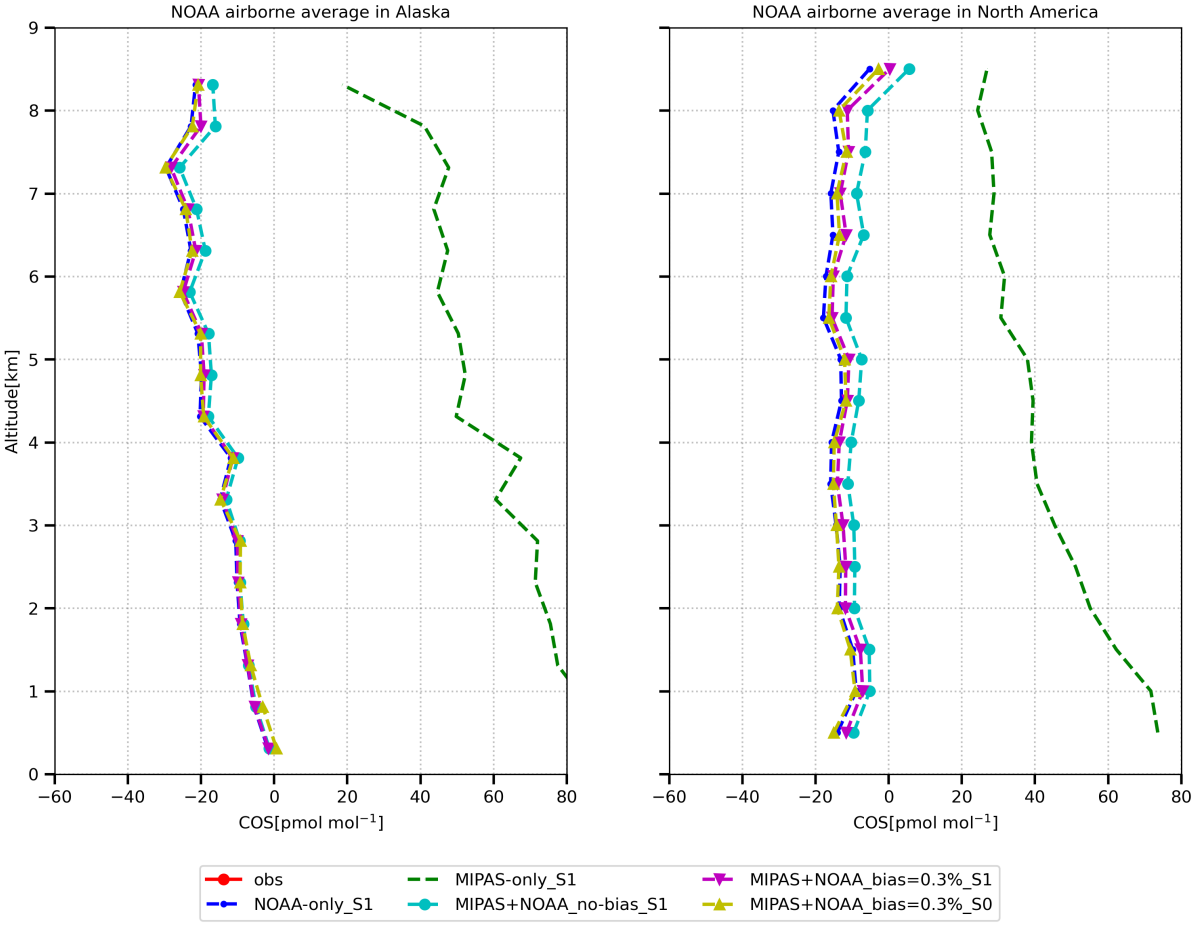

Figure S5. Differences between NOAA airborne observations and inversions. The differences are model sampled profiles minus NOAA airborne observations. The profiles were averaged each 500 m vertically and grouped into two regions, Alaska and North America.

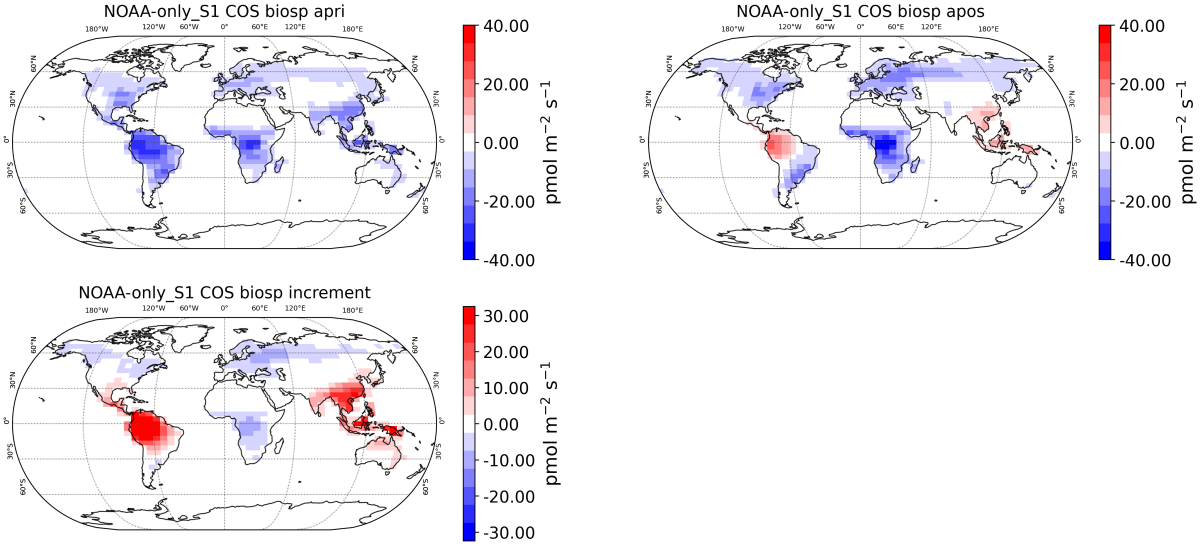

Figure S6. The prior, posterior and increment of the biosphere flux in inversion NOAA-only_S1. The flux represents the annual mean of 2009.

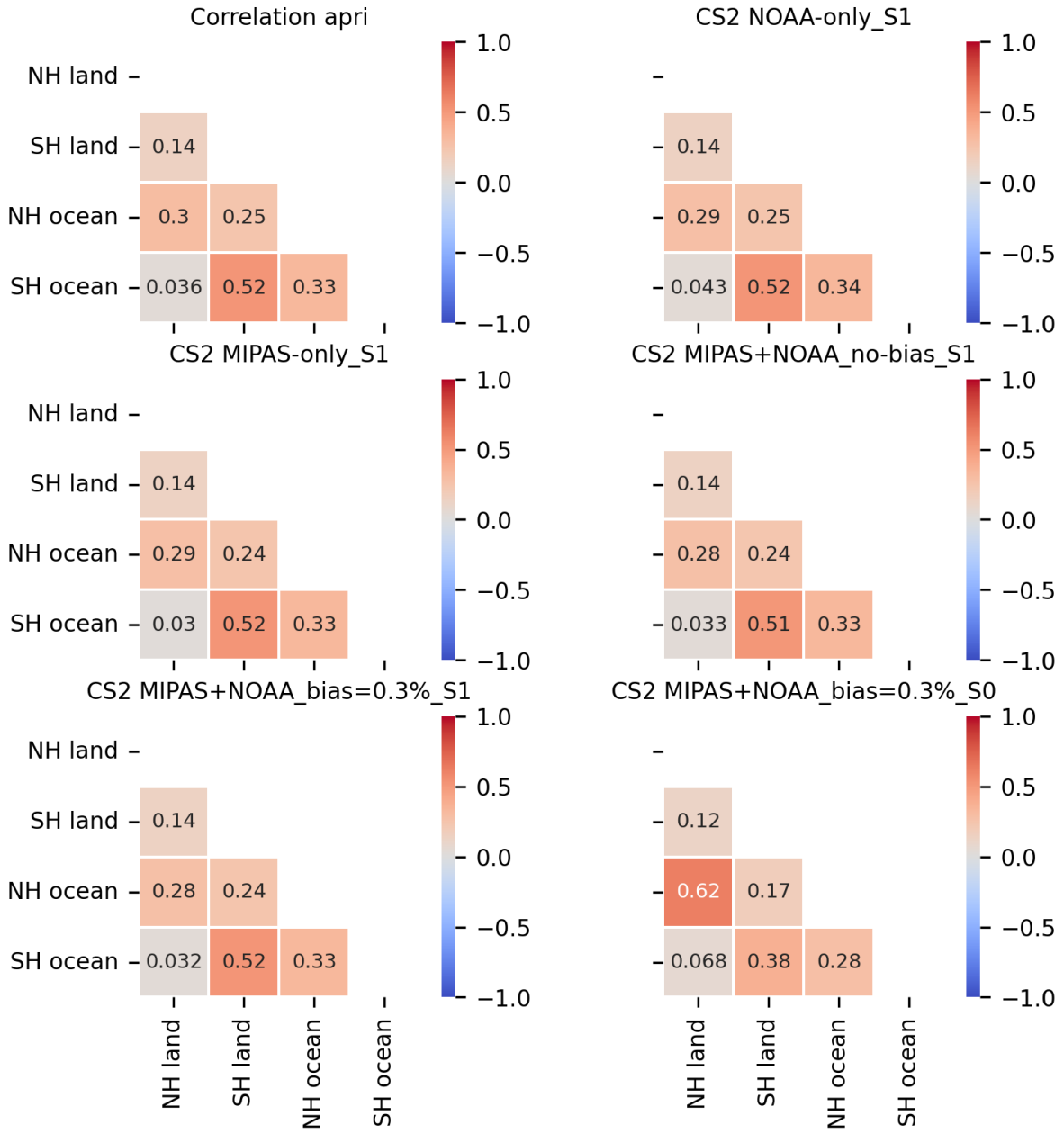

Figure S7. Aggregated prior and posterior correlations of the total CS_2 flux between different regions (NH lands and oceans, SH lands and oceans). The top left penal is the prior correlation between the regions, and the other inversions are the posterior correlations for the different inversions. The CS_2 total flux is the sum of anthropogenic and oceanic fluxes.

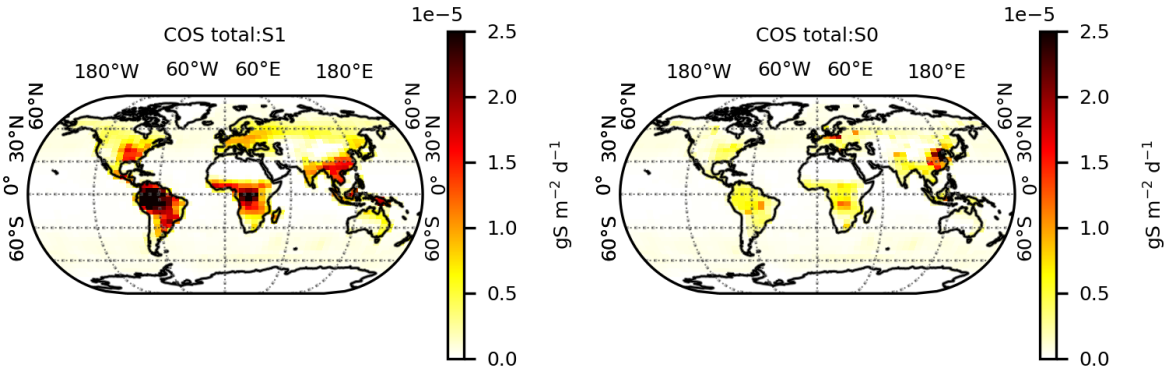

Figure S8. The prior error of the total COS flux for scenario S1 (left) and S0 (right) on grid level. The total COS flux is the sum of anthropogenic, oceanic, biomass burning and biosphere fluxes.

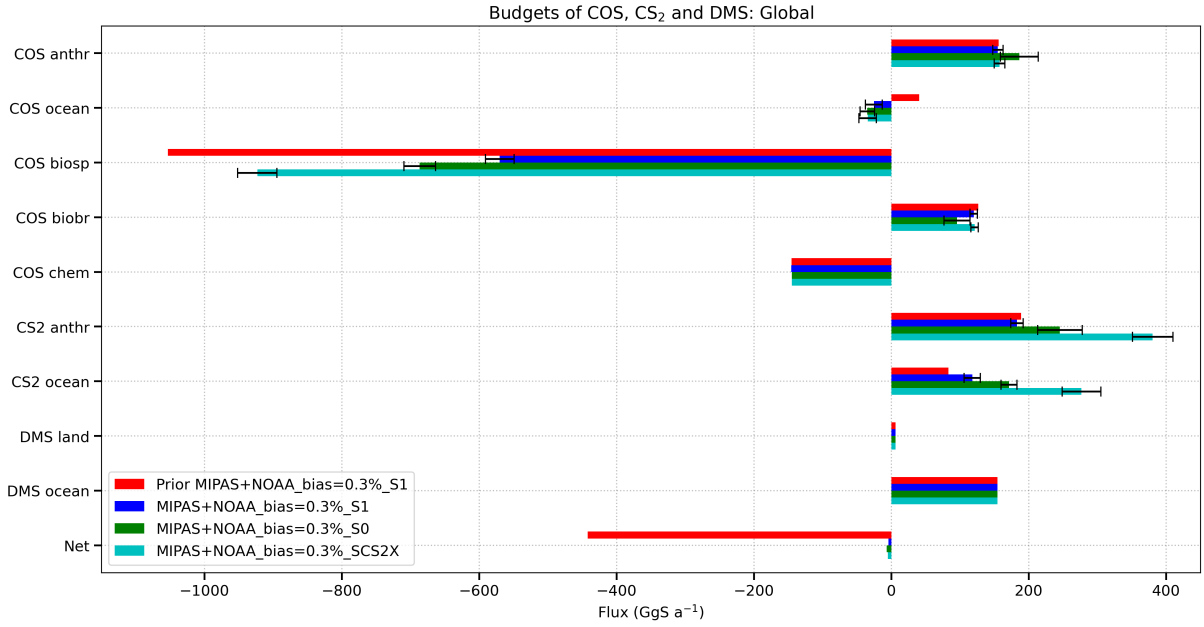

Figure S9. Global COS budgets for the inversions using NOAA and MIPAS data and applying bias correction. The error setting of the additional SCSX2 scenario was: biosphere 10%, ocean COS 50%, ocean CS_2 150%, biomass burning 10%, anthropogenic COS 10%, anthropogenic CS_2 150%, and DMS is not optimized. The error bars represent the prior or posterior errors which are aggregated to the global scale. Note that the prior errors on the fluxes are not plotted because scenarios S1 and SCSX2 have different prior errors. Note further that the CS_2 and DMS budget terms are counted as indirect COS fluxes.

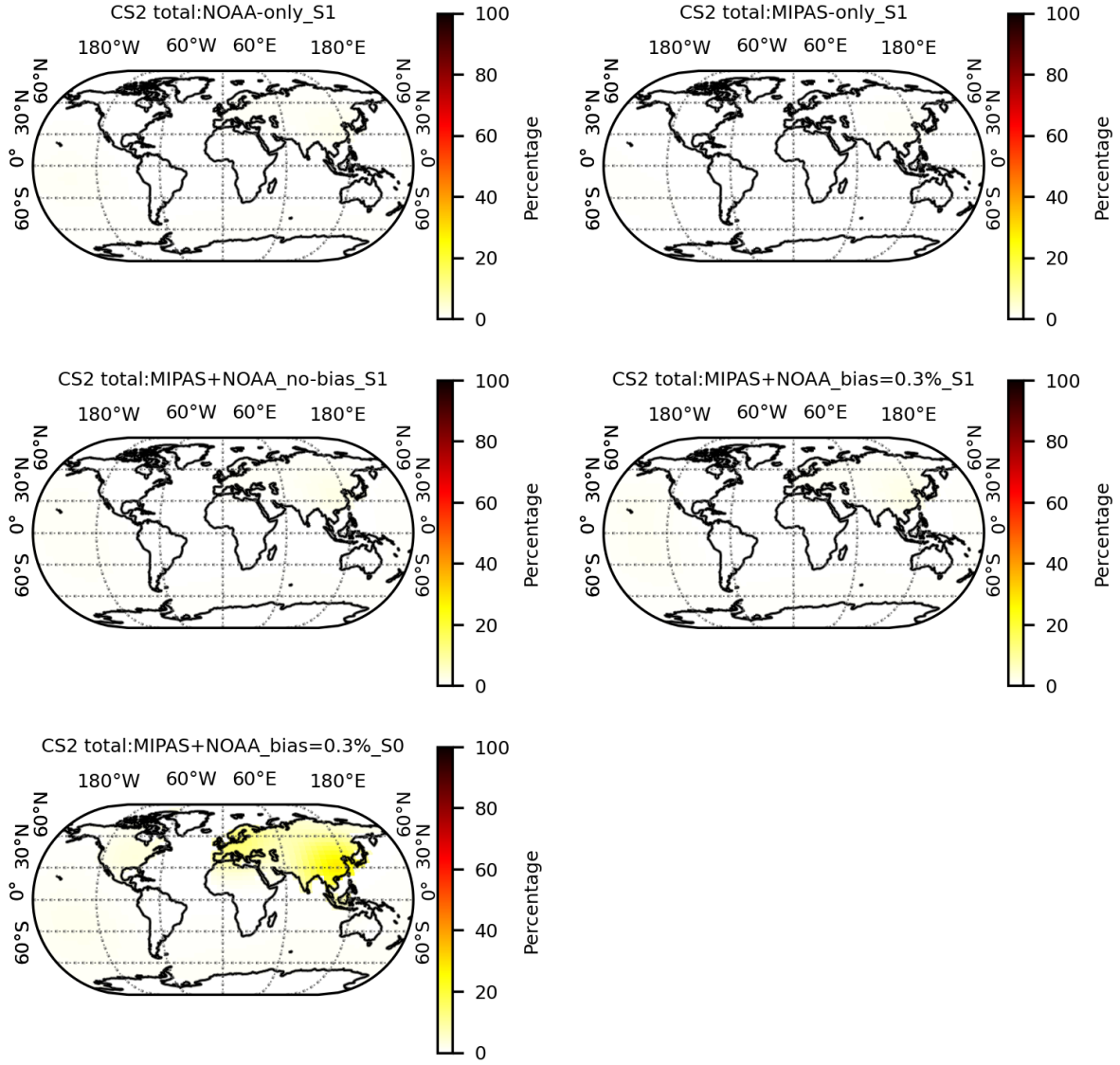

Figure S10. Error reduction of the total CS_2 flux at the grid scale for the different inversions. The total CS_2 flux is the sum of anthropogenic and oceanic fluxes.

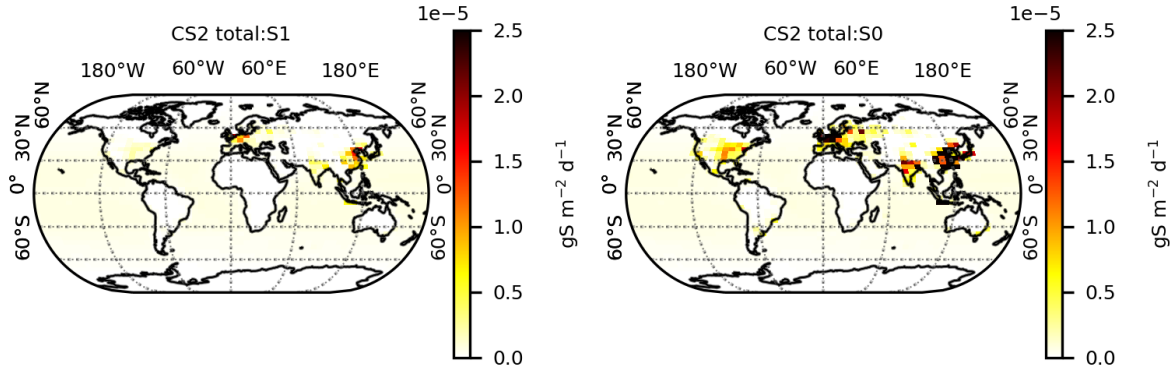

Figure S11. Prior error of the total CS_2 flux at the grid scale for the different inversions. The total CS_2 flux is the sum of anthropogenic and oceanic fluxes.